The Ti₃AlC₂ MAX Phase as an Efficient Catalyst for Oxidative Dehydrogenation of n-Butane

Wesley H. K. Ng, Edwin S. Gnanakumar, Erdni Batyrev, Sandeep K. Sharma, Pradeep K. Pujari, Heather F. Greer, Wuzong Zhou, Ridwan Sakidja, Gadi Rothenberg, Michel W. Barsoum,* and N. Raveendran Shiju*

Abstract: *Dehydrogenation or oxidative dehydrogenation (ODH) of alkanes to produce alkenes directly from natural gas/shale gas is gaining in importance. Ti₃AlC₂, a MAX phase, which hitherto had not been used in catalysis, efficiently catalyzes the ODH of n-butane to butenes and butadiene, which are important intermediates for the synthesis of polymers and other compounds. The catalyst, which combines both metallic and ceramic properties, is stable for at least 30 h on stream, even at low O₂:butane ratios, without suffering from coking. This material has neither lattice oxygens nor noble metals, yet a unique combination of numerous defects and a thin surface $Ti_{1-y}Al_yO_{2-y/2}$ layer that is rich in oxygen vacancies makes it an active catalyst. Given the large number of compositions available, MAX phases may find applications in several heterogeneously catalyzed reactions.*

MAX phases, a term coined in the late 1990s, are a family of ternary carbides and nitrides with layered hexagonal crystal structures. Their name reflects their chemical formula: $M_{n+1}AX_n$, where M is an early transition metal, A is an element (mostly from Groups 13 and 14), X is carbon and/or nitrogen, and $n = 1$, 2, or 3 (see Figure 1). Most of these phases were discovered in powder form already in the 1960s, though the synthesis of phase-pure bulk samples was only achieved in 1996.[1] The MAX phases are interesting because they exhibit a unique combination of ceramic and metallic properties.[2–4] Their bonding is a combination of covalent and metallic.[5] The density of states at the Fermi level is substantial and dominated by the d–d orbitals of the M-element.[5] Similarly, their electrical resistivity is metal-like in that it drops linearly with decreasing temperatures. They
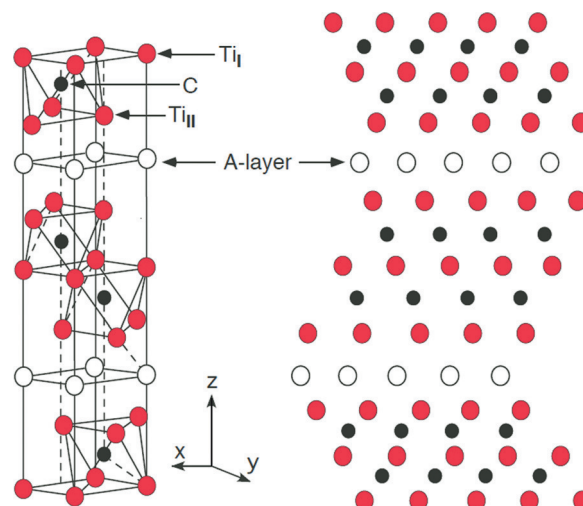
Figure 1. Hexagonal crystal structure of a 312 MAX phase. Ti atoms have two different sites, denoted Ti_I and Ti_II. Every fourth layer is interleaved with layers of pure A-group element.

conduct heat and electricity like metals, yet they are elastically stiff, strong, brittle, and some are heat-tolerant like ceramics.[6]

Numerous studies have been published on the electrical, thermal and mechanical properties of the MAX phases.[7–12] However, to the best of our knowledge, no catalytic applications have been reported so far. Considering the combination of metallic and ceramic properties and high stability, we anticipated that these materials could be good catalysts. Moreover, the fact that they differ from most conventional

[*] W. H. K. Ng, Dr. E. S. Gnanakumar, Prof. Dr. G. Rothenberg, Dr. N. R. Shiju
Van't Hoff Institute for Molecular Sciences, University of Amsterdam
P.O. Box 94157, 1090GD Amsterdam (The Netherlands)
E-mail: n.r.shiju@uva.nl

Dr. E. Batyrev
Tata Steel, R&D
Ijmuiden (The Netherlands)

Dr. S. K. Sharma, Dr. P. K. Pujari
Radiochemistry Division, Bhabha Atomic Research Centre
Mumbai 400 085 (India)

Dr. H. F. Greer, Prof. Dr. W. Z. Zhou
School of Chemistry, University of St Andrews
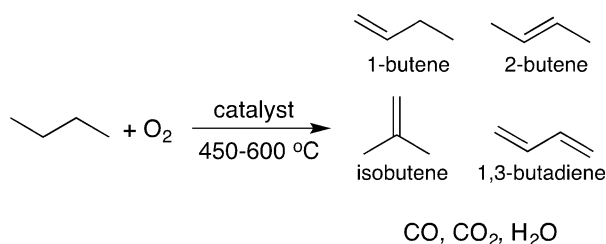St Andrews KY16 9ST (UK)

Dr. R. Sakidja
Dept. of Physics, Astronomy and Materials Science
Missouri State University
901 South National Ave., Springfield, MO 65897 (USA)

Prof. Dr. M. W. Barsoum
Drexel University, Department of Materials Science & Engineering,
Philadelphia, PA 19104 (USA)
E-mail: barsoumw@drexel.edu

catalytic materials (because they are neither oxides nor pure metals) triggered our curiosity. Such different materials may open reaction pathways that are unavailable to traditional catalysts.

Considering the layered structure with alternating metals and non-metals and thermal stability, we opted to study the catalytic application of MAX phases in oxidative dehydrogenation (ODH).[13–18] Specifically, we examined the oxidative dehydrogenation of butane to butenes and 1,3-butadiene (Scheme 1). Butenes, and especially butadiene, are important

Table 1: Performance of the Ti_3AlC_2 in butane ODH.

O_2/butane molar ratio[a]	Butane conversion [%]	Total selectivity of butenes [%]	Selectivity of 1,3-BD [%]	Selectivity of propene [%][b]
0.25:1	10.1	35.0	25.0	1.2
0.5:1	20.3	29.0	21.0	1.4
1:1	24.2	27.0	19.5	1.7
1:1[c]	13.8	20.7	16	1.6

[a] Reaction conditions: temperature = 550°C; flow rate = 17 mL min^{-1}; catalyst = 0.1 g; total pressure = 1 bar. [b] Trace amounts of ethylene and methane were also produced. The remainder is CO and CO_2. [c] Temperature = 500°C.

Scheme 1. The catalytic oxidative dehydrogenation of butane to give butenes, butadiene, CO, and CO_2.

industrial precursors for producing synthetic rubbers and plastics. This reaction has recently gained importance with the advent of shale gas and the increased use of natural gas as a cleaner carbon source.[15, 19–29] The problem is that the typical conditions that can activate alkanes often lead to low alkene selectivity, because the products are oxidized further to CO and CO_2. We now report the discovery that Ti_3AlC_2, a commercially available MAX phase, is a highly active and selective catalyst for butane ODH. It gives high yields of C4 alkenes, especially 1,3-butadiene.

We synthesized the Ti_3AlC_2 MAX phase by a ceramic synthesis route and confirmed its structure by X-ray diffraction (see the Supporting Information for full experimental details). It consists of a c-axis stacking sequence where two layers of edge sharing CTi_6 octahedra are sandwiched between planar layers of Al. The butane ODH study with Ti_3AlC_2 was carried out at different temperatures, varying the O_2:butane ratio from 0.25:1 up to 1:1. The product mixture contained 1-butene, 2-butene, butadiene, propene, CO_2, and CO. Control experiments without a catalyst yielded <1% of alkenes. At an O_2/butane ratio of 0.25:1 and 550°C, Ti_3AlC_2 gave nearly 35% selectivity for butenes and 25% selectivity for butadiene at 10% conversion (Table 1). At higher O_2/butane ratios of 0.5 and 1, conversion increased to 20% and 24%, respectively, without significant loss in selectivity for butenes and butadiene. Even at 24% conversion, the partial oxidation (butenes + butadiene) selectivity is close to 50%, which is remarkable. The catalyst is stable, retaining its selectivity during a long-time test (Supporting Information, Figure S1). XRD analysis after the reaction did not show any major structural changes further confirming the stability of the phase (Supporting Information, Figure S2).

Such high selectivity for butadiene is rarely achieved in butane ODH. At the same conversion of butane, Ti_3AlC_2 was more selective for butenes and butadiene than $Mg_3V_2O_8$ or

$Mg_3V_2O_7$, that are amongst the best catalysts reported so far for this reaction.[29] Remarkably our Ti_3AlC_2 catalyst was still active and stable at O_2:butane ratios ≤1:1 (see Table 1; Supporting Information, Figure S1). Typical metal oxide catalysts require ratios ≥2:1 to prevent severe deactivation due to coke deposition.[29]

The initial steps of the ODH reaction (O_2 and alkane activation) normally follow a Mars–Van Krevelen mechanism for metal oxides, wherein the lattice oxygen is the reactive species. This means that the activity of metal oxide catalysts towards hydrocarbons depends on the strength of the metal–oxygen bond of the catalyst. In our case, there are no bulk lattice oxygen atoms available, making the adsorption of oxygen on the catalyst surface to generate active oxygen species inevitable for the reaction to occur. This adsorption depends strongly on the defect sites at the catalyst surface. High-resolution transmission electron microscopy (HRTEM) analysis indeed showed that the catalyst particles contain many defects, most commonly domain, point, and layered defects (Figure 2). These defects might act as adsorption as well as reaction sites. Positron annihilation lifetime spectroscopic investigation (PALS) of our catalyst showed two positron lifetime components (Supporting Information, Table S1 and Figure S3), which are higher than the bulk positron lifetime in titanium carbide (107 ps), indicating positron annihilation from defect sites.[30] The first lifetime component (189.7 ± 6.1 ps) is very close to the positron lifetime for monovacancy of Ti, indicating the existence of Ti vacancy defects. The second lifetime component (300.9 ± 9 ps) is attributed to defects with a larger open volume, such as vacancy clusters and voids. This agrees well with the HRTEM observation of layered defects. Trapping of positron in these defects will lead to a higher lifetime value. The corresponding intensities of the positron lifetime components indicate that concentration of mono vacancy defects are higher than the layer defects. HRTEM further shows a thin amorphous layer (5–10 nm) on the surface (Figure 2a), which according to EDX spectra contains a very high oxygen content compared to the inner bulk material (Supporting Information, Figure S4). The X-ray from oxygen has very low energy and can be easily absorbed so the oxygen content in the EDX spectrum may not be accurate, therefore quantitative data analysis is not provided. Further confirmation of a high oxygen content in the amorphous surface layer was provided through EDX elemental mapping (Figure 3).
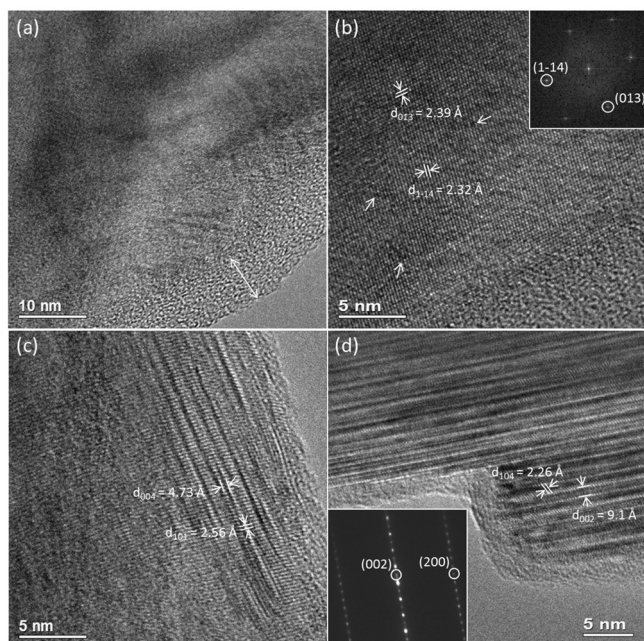
Figure 2. HRTEM images of Ti₃AlC₂. a) A thin pale contrasted amorphous surface layer (marked by arrow). b) Higher magnification image of a selected area in (a) showing many point defects (marked by arrows). c) Image showing many disordered layer defects. d) Image showing many partially ordered layer defects. Inset: the corresponding SAED pattern. The marked d-spacings are indexed to the unit cell of Ti₃AlC₂.
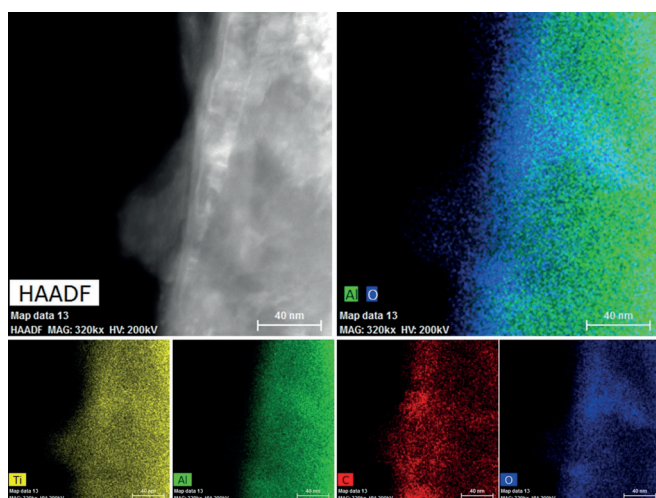
Figure 3. HAADF STEM image (top left) and elemental maps for Al + O (top right) and Ti, Al, C, and O on the Ti₃AlC₂ MAX phase (bottom).

Based on the analysis of EDX spectra and mapping, we reason that the thin layer on the catalyst surface is a mixed oxide of Al and Ti. Alternatively, it may be pure alumina or alumina/titania but this appears to be less likely according to our EDX mapping data. We believe that this thin layer, coupled with the large electron reservoir below it, holds the key to the catalytic activity.[31] To confirm this, we studied the catalyst by XPS (see Figure 4), which has indeed proved that, besides the individual carbide peaks, the surface has a signifi-
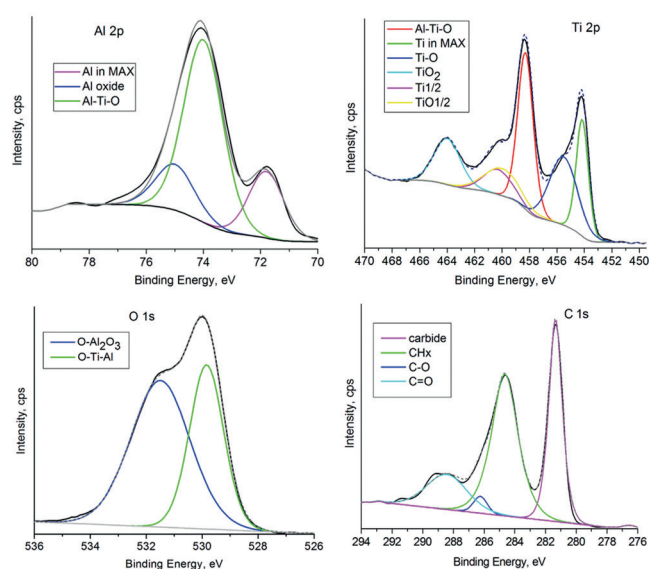
Figure 4. Al 2p, Ti 2p, O 1s, and C 1s XPS of Ti₃AlC₂, showing different types of possible species on the surface. Besides individual carbides and oxides, the surface has a significant amount of mixed oxide (Al-Ti-O).

cant amount of mixed oxides as well as oxidized Al and Ti. This supports our hypothesis that the surface layer observed by TEM is a mixed Al-Ti-O. Alumina and titania can form a solid solution with the formula, $(Ti_{1-y}Al_y)O_{2-y/2}$, creating a mole of oxygen vacancies for every two moles of alumina that is added. Previous studies indicated that, after high temperature oxidation, a $(Ti_{1-y}Al_y)O_{2-y/2}$ layer is formed on the surface of Ti₃AlC₂.[32,33] It is reasonable to assume that the oxygen vacancies should also act as active oxygen creators from gas phase oxygen, which can explain the catalytic activity. The adsorbed oxygen species formed upon activation of gas-phase O₂ on surface oxygen vacancies can activate n-butane. These species are most likely monoatomic, and therefore more selective for partial oxidation.[28]

We used N₂O chemisorption coupled with XPS analysis to estimate the concentration of oxygen vacancies using the fact that metallic sites will split adsorbed N₂O at required activation temperature, leading to the oxidation of metal to metal oxide.[34] Thus, we first reduced the Ti₃AlC₂ MAX phase in UHV (10^{-7} mbar) at 500°C, creating oxygen vacancies and subsequently exposed the reduced surface to N₂O. We then examined the re-oxidized surface by XPS. The amount of Ti that undergoes oxidation can be estimated by linear extrapolation of the subsurface (diffusion-dependent oxidation) uptake to $t = 0$ (Supporting Information, Figure S5),[35] which gives 3.5 at %. The corresponding oxygen amount is 7.0 at %. Using this, we can estimate the concentration of oxygen vacancies as 9×10^{26} m⁻³ (see the Supporting information and Figure S6 for more details).

To further prove the role of oxygen vacancies, we also tested another MAX phase Ti₃SiC₂, isostructural with Ti₃AlC₂ wherein the Al layers are replaced by Si.[1] The difference here is that unlike alumina and titania, silica and titania do not form a solid solution. Hence, if our hypothesis that the

$(Ti_{1-y}Al_y)O_{2-y/2}$ layer is responsible for the catalysis, Ti_3SiC_2 should be much less selective in ODH. A series of control experiments at varying temperatures proved that to be true. Ti_3SiC_2 gave lower conversion (from 4% at 450°C up to 16% at 600°C compared to 24% at 550°C for Ti_3AlC_2) and the total yield of butene and butadiene was only 1–2% (Supporting Information, Table S2). This confirms that the lack of sufficient anion vacancies in Ti_3SiC_2 due to its inability to form a non-stoichiometric surface oxide layer leads to non-selective oxidation in this case. Kondratenko et al. recently reported enhanced selectivity for propene in non-oxidative dehydrogenation of propane by deliberately increasing the concentration of defect sites in unconventional oxide catalysts.[36] They promoted ZrO_2, which has an unchangeable oxidation state, with other metal oxides, which created lattice defects consisting of coordinatively unsaturated Zr cations. Our results further confirm that the defective structure in unconventional materials can generate unexpected catalytic properties. Moreover, stable activity and selectivity over several hours (Supporting Information, Figure S1) indicate high surface mobility of oxygen anions and consequent rapid reoxidation, which is apparently due to the layered structure of our Ti_3AlC_2 MAX phase. Since adsorption of butane on the surface should influence the reaction, we also compared the relative adsorption of n-butane on both samples at 250°C (highest temperature possible in our adsorption equipment). These experiments showed that Ti_3AlC_2 adsorbs significantly more n-butane than Ti_3SiC_2 (Supporting Information, Figure S7), which is apparently due to the defective structure.
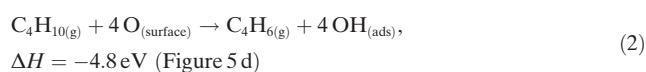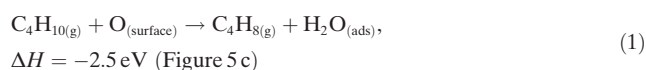
To understand further the experimental observations, we evaluated computationally a number of scenarios of favorable chemical reactions at the surface. Note that this is not an exhaustive search. Since a previous equilibrium study has shown that a stable ternary phase of Al_2TiO_5 exists in the Ti-Al-O system,[37,38] we used the O-terminating (001) surface of this phase as a simple model to represent the mixed-cation oxide surface on Ti_3AlC_2. We performed electronic structure calculations as implemented in the density functional theory approximation (VASP ab initio code[39]) to assess the energetics of the adsorption of butane onto the oxygen-terminating surface at the ground state (at 0 K). Further details of the method, exchange-correlation potentials used (PAW-PBE[40]), and convergence criteria (electronic convergence criterion of 10^{-5} eV and force convergence limit of 10^{-2} eV/A) are given elsewhere.[41,42] A list of chemical reactions along with the final atomic configurations are given in the Supporting Information, Table S3.

The results show that butane adsorbs relatively easily, through the formation of a C−O bond on the selected surface. This is followed immediately by the dissociation of a hydrogen atom onto the surface, captured by one of the dangling bonds of oxygen: $C_4H_{10(g)} + O_{(surface)} \rightarrow C_4H_{9(ads)} + OH_{(ads)}$; $\Delta H = -2.99$ eV. Figure 5a shows the resulting atomic configuration (a video showing the relaxation sequence is included in the Supporting Information). This reaction releases roughly 3 eV per molecule of butane. A possible subsequent reaction where by the adsorbed C_4H_9 further decomposes into $C_4H_{8(ads)}$ by releasing another hydrogen atom forming a water molecule (Figure 5b) is also favored, for an overall chemical reaction
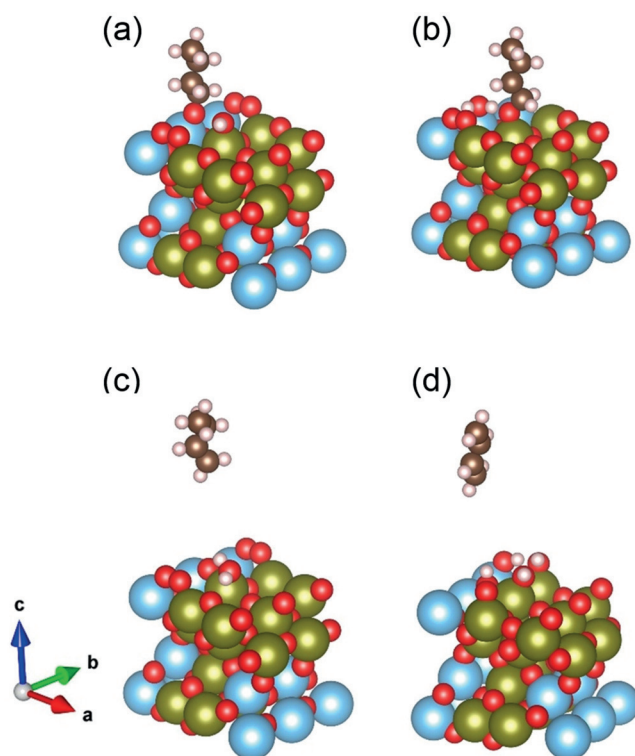
Figure 5. Atomic configurations of various steps of butane interaction with the MAX surface, taking Al_2TiO_5 as a model resulting in a) $C_4H_{9(ads)} + OH_{(ads)}$, b) $C_4H_{8(ads)} + H_2O_{(ads)}$, c) $C_4H_{8(ads)} + H_2O_{(ads)}$, and d) $C_4H_{6(g)} + 4OH_{(ads)}$. See the Supporting Information for more details. Ti blue, O red, Al gold.

of: $C_4H_{10(g)} + O_{(surface)} \rightarrow C_4H_{8(ads)} + H_2O_{(ads)}$; $\Delta H = -3.35$ eV. A further oxidative dehydrogenation may be facilitated by the release of more hydrogen atoms from the adsorbed C_4H_8 yielding 1,3-butadiene according to: $C_4H_{8(ads)} + O_{(ads)} \rightarrow C_4H_{6(ads)} + H_2O_{(ads)}$; $\Delta H = -1.39$ eV. Overall, releasing two or four hydrogen atoms from butane onto the surface yielding adsorbed water molecule/forming OH bonds is favorable on the Al_2TiO_5 surface [Equations (1) and (2)]:

$$C_4H_{10(g)} + O_{(surface)} \rightarrow C_4H_{8(g)} + H_2O_{(ads)},$$
$$\Delta H = -2.5 \text{ eV (Figure 5c)} \tag{1}$$

$$C_4H_{10(g)} + 4O_{(surface)} \rightarrow C_4H_{6(g)} + 4OH_{(ads)},$$
$$\Delta H = -4.8 \text{ eV (Figure 5d)} \tag{2}$$

As shown in the Supporting Information, Reaction (S2), the overall desorption reaction $C_4H_{10(g)} \rightarrow C_4H_{9(g)} + H_{(ads)}$ is slightly endothermic, with $\Delta H = 0.9$ eV. This value however is much lower than the energy required for releasing the intermediate product of $C_4H_{9(ads)}$ into $C_4H_{9(g)}$ ($\Delta H = +3.89$ eV). Thus, both types of direct dissociation will not be the easiest pathways and thus, other intermediate mechanisms must have taken place to lower these overall energy barrier. This gives credence to the possible role of oxygen defects and/or a higher operating temperature to enable the reaction to proceed. Nevertheless, the overall reactions involving further dissociations do indicate energetically favorable conditions for oxidative dehydrogenation of

butane on a mixed Al-Ti-O surface into butane and butadiene.

In conclusion, there is no lattice or structural oxygen in the Ti₃AlC₂ MAX phase, and it does not contain any noble metals, yet its unique combination of defects and very thin, presumably non-stoichiometric, oxide surface layer containing oxygen vacancies resulted in O-containing active sites and made this material catalytically active. Given the interesting set of properties that the MAX phases exhibit, especially their high-temperature stability, metallic, and ceramic properties as well as low cost, our work has very wide scope in heterogeneous catalysis. For an industrial process, we still need to resolve issues such as product separation and high recycle rate; however, we believe that our results will open new fundamental studies of MAX phases. There are over 60 MAX phases synthesized so far, with very different compositions. The unique properties of these materials as catalysts or catalyst supports in suitable reactions are waiting to be explored.

Conflict of interest

The authors declare no conflict of interest.

Keywords: butadiene · heterogeneous catalysis · natural gas · oxidative dehydrogenation · shale gas

How to cite: *Angew. Chem. Int. Ed.* **2018**, *57*, 1485–1490
Angew. Chem. **2018**, *130*, 1501–1506

[1] M. W. Barsoum, T. ElRaghy, *J. Am. Ceram. Soc.* **1996**, *79*, 1953–1956.

[2] Y. Gogotsi, A. Nikitin, H. H. Ye, W. Zhou, J. E. Fischer, B. Yi, H. C. Foley, M. W. Barsoum, *Nat. Mater.* **2003**, *2*, 591–594.

[3] M. W. Barsoum, T. Zhen, S. R. Kalidindi, M. Radovic, A. Murugaiah, *Nat. Mater.* **2003**, *2*, 107–111.

[4] H. I. Yoo, M. W. Barsoum, T. El-Raghy, *Nature* **2000**, *407*, 581–582.

[5] N. Medvedeva, D. Novikov, A. Ivanovsky, M. Kuznetsov, A. Freeman, *Phys. Rev. B* **1998**, *58*, 16042–16050.

[6] S. Aryal, R. Sakidja, M. W. Barsoum, W.-Y. Ching, *Phys. Status Solidi B* **2014**, *251*, 1480–1497.

[7] M. W. Barsoum, *MAX Phases: Properties of Machinable Carbides and Nitrides*, Wiley-VCH, Weinheim, **2013**.

[8] H. Ding, N. Glandut, X. Fan, Q. Liu, Y. Shi, J. Jie, *Int. J. Hydrogen Energy* **2016**, *41*, 6387–6393.

[9] H. Zhang, C. Zhang, T. Hu, X. Zhan, X. Wang, Y. Zhou, *Sci. Rep.* **2016**, *6*, 23943.

[10] W. G. Sloof, R. Pei, S. A. McDonald, J. L. Fife, L. Shen, L. Boatemaa, A.-S. Farle, K. Yan, X. Zhang, S. van der Zwaag, P. D. Lee, P. J. Withers, *Sci. Rep.* **2016**, *6*, 23040.

[11] S. C. Middleburgh, G. R. Lumpkin, D. Riley, *J. Am. Ceram. Soc.* **2013**, *96*, 3196–3201.

[12] M. Naguib, M. Kurtoglu, V. Presser, J. Lu, J. Niu, M. Heon, L. Hultman, Y. Gogotsi, M. W. Barsoum, *Adv. Mater.* **2011**, *23*, 4248–4253.

[13] C. Caro, K. Thirunavukkarasu, M. Anilkumar, N. R. Shiju, G. Rothenberg, *Adv. Synth. Catal.* **2012**, *354*, 1327–1336.

[14] J. H. Blank, J. Beckers, P. F. Collignon, F. Clerc, G. Rothenberg, *Chem. Eur. J.* **2007**, *13*, 5121–5128.

[15] N. Madaan, R. Haufe, N. R. Shiju, G. Rothenberg, *Top. Catal.* **2014**, *57*, 1400–1406.

[16] E. V. Ramos-Fernandez, N. J. Geels, N. R. Shiju, G. Rothenberg, *Green Chem.* **2014**, *16*, 3358–3363.

[17] a) N. R. Shiju, M. Anilkumar, S. P. Gokhale, B. S. Rao, C. V. V. Satyanarayana, *Catal. Sci. Technol.* **2011**, *1*, 1262–1270; b) N. R. Shiju, V. V. Guliants, *ChemPhysChem* **2007**, *8*, 1615–1617.

[18] G. Rothenberg, E. A. de Graaf, A. Bliek, *Angew. Chem. Int. Ed.* **2003**, *42*, 3366–3368; *Angew. Chem.* **2003**, *115*, 3488–3490.

[19] R. Bulánek, A. Kaluzova, M. Setnicka, A. Zukal, P. Cicmanec, J. Mayerova, *Catal. Today* **2012**, *179*, 149–158.

[20] H. Nguyen Ngoc, H. Ngo Duc, C. Le Minh, *Appl. Catal. A* **2011**, *407*, 106–111.

[21] M. Setnicka, R. Bulanek, L. Capek, P. Cicmanec, *J. Mol. Catal. A* **2011**, *344*, 1–10.

[22] N. Madaan, N. R. Shiju, G. Rothenberg, *Catal. Sci. Technol.* **2016**, *6*, 125–133.

[23] Z. Nawaz, F. Wei, *Ind. Eng. Chem. Res.* **2013**, *52*, 346–352.

[24] H. Nguyen Ngoc, H. Ngo Duc, C. Le Minh, *J. Mol. Model.* **2013**, *19*, 3233–3243.

[25] G. Raju, B. M. Reddy, S.-E. Park, *J. CO₂. Util.* **2014**, *5*, 41–46.

[26] V. Schwartz, W. Fu, Y.-T. Tsai, H. M. Meyer III, A. J. Rondinone, J. Chen, Z. Wu, S. H. Overbury, C. Liang, *ChemSusChem* **2013**, *6*, 840–846.

[27] M. Setnicka, P. Cicmanec, R. Bulanek, A. Zukal, J. Pastva, *Catal. Today* **2013**, *204*, 132–139.

[28] a) J. C. Védrine, *Catalysts* **2016**, *6*, 22; b) S. Furukawa, M. Endo, T. Komatsu, *ACS Catal.* **2014**, *4*, 3533–3542; c) B. Rabindran Jermy, S. Asaoka, S. Al-Khattaf, *Catal. Sci. Technol.* **2015**, *5*, 4622–4635; d) J. K. Lee, U. G. Hong, Y. Yoo, Y.-J. Cho, J. Lee, H. Chang, I. K. Song, *J. Nanosci. Nanotechnol.* **2013**, *13*, 8110–8115; e) D. Milne, T. Seodigeng, D. Glasser, D. Hildebrandt, B. Hausberger, *Catal. Today* **2010**, *156*, 237–245; f) J. C. Jung, H. Kim, Y. S. Kim, Y.-M. Chung, T. J. Kim, S. J. Lee, S.-H. Oh, I. K. Song, *Appl. Catal. A* **2007**, *317*, 244–249; g) J. Rischard, C. Antinori, L. Maier, O. Deutschmann, *Appl. Catal. A* **2016**, *511*, 23–30; h) M. Eichelbaum, M. Haevecker, C. Heine, A. Karpov, C.-K. Dobner, F. Rosowski, A. Trunschke, R. Schloegl, *Angew. Chem. Int. Ed.* **2012**, *51*, 6246–6250; *Angew. Chem.* **2012**, *124*, 6350–6354; i) M. E. Davis, C. J. Dillon, J. H. Holles, J. Labinger, *Angew. Chem. Int. Ed.* **2002**, *41*, 858–860; *Angew. Chem.* **2002**, *114*, 886–888; j) B. Solsona, F. Ivars, P. Concepcion, J. M. Lopez Nieto, *J. Catal.* **2007**, *250*, 128–138; k) Y. Dong, F. J. Keil, O. Korup, F. Rosowski, R. Horn, *Chem. Eng. Sci.* **2016**, *142*, 299–309; l) D. Lesser, G. Mestl, T. Turek, *Appl. Catal. A* **2016**, *510*, 1–10; m) S. D. Jackson, S. Rugmini, *J. Catal.* **2007**, *251*, 59–68; n) J. McGregor, Z. Huang, G. Shiko, L. F. Gladden, R. S. Stein, M. J. Duer, Z. Wu, P. C. Stair, S. Rugmini, S. D. Jackson, *Catal. Today* **2009**, *142*, 143–151.

[29] J. Zhang, X. Liu, R. Blume, A. Zhang, R. Schloegl, D. S. Su, *Science* **2008**, *322*, 73–77.

[30] M. J. Puska, M. Sob, G. Brauer, T. Korhonen, *Phys. Rev. B* **1994**, *49*, 10947–10957.

[31] J. Schäferhans, S. Gómez-Quero, D. V. Andreeva, G. Rothenberg, *Chem. Eur. J.* **2011**, *17*, 12254–12256.

[32] J. A. S. Ikeda, Y. M. Chiang, B. D. Fabes, *J. Am. Ceram. Soc.* **1990**, *73*, 1633–1640.

[33] M. W. Barsoum, *J. Electrochem. Soc.* **2001**, *148*, C544–C550.

[34] a) F. Kapteijn, J. Rodriguez-Mirasol, J. A. Moulijn, *Appl. Catal. B* **1996**, *9*, 25–64; b) E. D. Batyrev, J. C. van den Heuvel, J. Beckers, W. P. A. Jansen, H. L. Castricum, *J. Catal.* **2005**, *229*, 136–143.

[35] M. J. Luys, P. H. van Oefelt, W. G. J. Brouwer, A. P. Pijpers, J. F. F. Scholten, *Appl. Catal.* **1989**, *46*, 161.

[36] T. Otroshchenko, S. Sokolov, M. Stoyanova, V. A. Kondratenko, U. Rodemerck, D. Linke, E. V. Kondratenko, *Angew. Chem. Int. Ed.* **2015**, *54*, 15880–15883; *Angew. Chem.* **2015**, *127*, 16107–16111.

[37] S. Das, *J. Phase Equilib.* **2002**, *23*, 525–536.

[38] B. Morosin, R. W. Lynch, *Acta Crystallogr. Sect. A* **1972**, *28*, 1040–1046.

[39] G. Kresse, J. Furthmüller, *Phys. Rev. B* **1996**, *54*, 11169–11186.

[40] J. P. Perdew, K. Burke, M. Ernzerhof, *Phys. Rev. Lett.* **1996**, *77*, 3865–3868.

[41] N. Li, R. Sakidja, W.-Y. Ching, *JOM* **2013**, *65*, 1487–1491.

[42] N. Li, R. Sakidja, W.-Y. Ching, *Appl. Surf. Sci.* **2014**, *315*, 45–54.